



Preparation and study of pyridothienopyrazines and their Ruthenium(II) complexes: a new family of bidentate ligands

Antonio Fernández-Mato, José María Quintela ^{*}, Carlos Peinador ^{*}, Carlos Platas-Iglesias

Departamento de Química Fundamental, Facultad de Ciencias, Universidad da Coruña, Campus A Zapateira, 15008 A Coruña, Spain

ARTICLE INFO

Article history:

Received 2 December 2010

Received in revised form 13 January 2011

Accepted 22 January 2011

Available online 28 January 2011

Keywords:

Bidentate ligands

Heteroleptic Ru(II)-complexes

Pyridothienopyrazine

Friedländer condensation

Heterodinuclear complexes

ABSTRACT

The Friedländer condensation of 3-aminothieno[2,3-*b*]pyrazine-2-carboxaldehyde with either methyl ketones or carbocyclic and heterocyclic ketones leads to a family of new bidentate ligands containing a pyridothienopyrazine coordinating unit. Complexation with [Ru(bpy)₂Cl₂] affords the corresponding six-coordinated Ru(II) complexes. The structures were analyzed by ¹H NMR spectroscopy, which shows shielding effects reflecting significant interligand π-stacking interaction in the complexes. The photochemical properties of the ligands and their metallic complexes have been also examined.

© 2011 Elsevier Ltd. All rights reserved.

1. Introduction

Heteroaromatic rings are important constituents of drugs and bioactive molecules. In addition, they have also received wide attention because of their ability to function as effective ligands to couple metal centers in a covalent manner resulting in polynuclear complexes that often possess new and interesting properties. Heteroaromatic nitrogen ligands have found wide applications on the new generation of molecules with extended applications in several important research and technological fields, including bioactive drugs, nonlinear optical materials, and other applications in optoelectronic devices.¹ In recent years, numerous efforts have been undertaken to develop efficient and selective methods for the preparation of polydentate ligands suitable for self-assembly processes.² Many of these ligands have been bi- or tri-dentate chelators in which a pyridine ring is the coordinating unit. Thus, two of the most extensively studied bidentate ligands employed in coordination chemistry are 2,2'-bipyridine (bpy) and 1,10-phenanthroline (phen) (Fig. 1). The latter may be considered as a 3,3'-etheno-bridged derivative of the former. The steric requirements of both ligands are very similar, and differences in the properties of their metal complexes may be mostly attributed to electronic differences arising from the greater electronegativity of phen.³ These ligands and related *N*-heterocycles are widely employed as metal-binding components in all aspects of coordination chemistry, and in

many of its modern applications to areas, such as supramolecular and bioinorganic chemistry.⁴ The tripyridyl analogue of bpy, which behaves as a tridentate chelator but enjoys many of the same coordination properties as bpy.⁵

Currently, an increasing important area of ligand design involves the synthesis and study of new photochemically active ligands and their use as chelating ligands.⁶ Indeed, linearly fused heteroacenes occupy a prominent position of research in π-conjugated small molecules because of their attractive electronic and optical properties.⁷ Among these heteroacenes, sulfur or/and nitrogen atoms are introduced widely to tune the solid-state structure and electronic structure of organic semiconductors while overcoming some drawbacks of acenes, such as low solubility and instability.⁸ Recently, we reported the synthesis and examination of the electronic absorption and emission spectra of new 2-[1,8]naphthyridinyl and

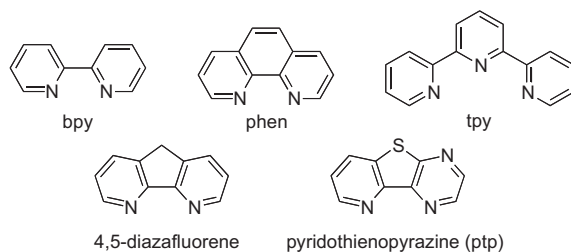


Fig. 1. Structures of bidentate and tridentate ligands.

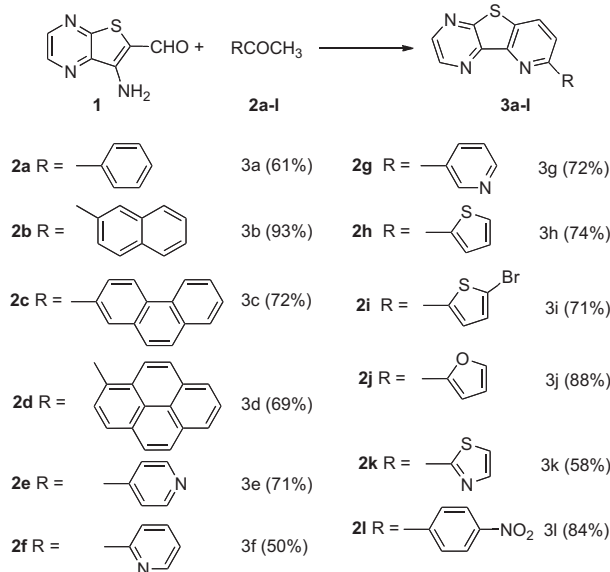
* Corresponding authors. E-mail address: carlos.peinador@udc.es (C. Peinador).

bis(2-[1,8]naphthyridinyl) fused ligands with multidentate binding sites.⁹ On the basis of such precedents, and as part of a programme of investigating the synthesis and study of new heterocyclic ligands¹⁰ and their use in coordination and supramolecular chemistry and self-assembly processes,¹¹ here we report the synthesis and a comprehensive study on the photophysical properties of a family of new bidentate ligands. That triheterocyclic pyridotheniopyrazine chelator ligand skeleton ptp (Fig. 1) may be considered as a 6,6'-sulfur-bridged aza-analogue of bpy and is expected to be applicable as appropriate chelating ligand in various photomaterials. To the best of our knowledge, this is the first report of bipyridine-, phenanthroline-, or 4,6-diazafluorene-like ligands with a sulfur-bridging atom. A simple and straightforward synthesis of the ligands has therefore been developed and the target compounds have been characterized in detail. The electronic properties have been studied by using electronic absorption and emission spectroscopy. The photophysical properties of their metallic complexes have been also examined.

2. Results and discussion

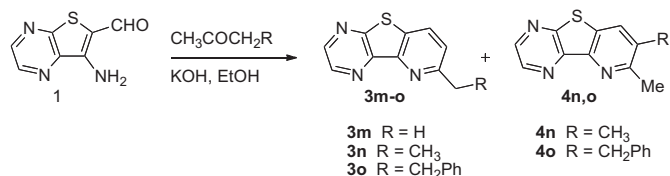
2.1. Synthesis

Amino carbonyl compounds are important building blocks in the synthesis of nitrogen-containing products, and are widely used by chemists in heterocyclic chemistry and in the pharmaceutical industry. The Friedländer reaction is still one of the simplest methods for the preparation of a variety of annulated and bisannulated pyridines.¹² In its most general form, the Friedländer reaction is the base- or acid-promoted condensation of an aromatic 2-amino-substituted carbonyl compound with an appropriately substituted carbonyl derivative containing a reactive α -methylene group followed by cyclodehydration.¹³ To make the title condensed pyridotheniopyrazine ligands accessible in large quantities, we have devised a simple and convenient synthesis starting from 3-aminothieno[2,3-*b*]pyrazine-2-carboxaldehyde **1**.¹⁴ The initial objective starts with the preparation of 2-aryl and 2-heteroaryl ligands **3a–l**. To this end, the base-catalyzed reaction of the aminoaldehyde **1** with aryl and heteroaryl ketones **2a–l** provides the corresponding 8-aryl and 8-heteroarylpyrido[2',3':4,5]thieno[2,3-*b*]pyrazine derivatives **3a–l** in acceptable to very good yields of 50–93% (Scheme 1).



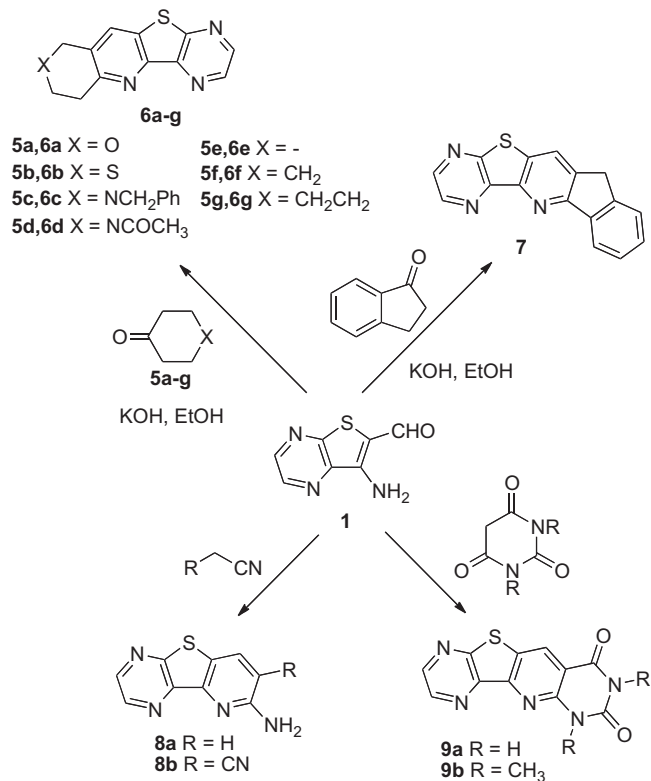
Scheme 1. Synthesis of pyridotheniopyrazines **3a–l** via Friedländer annulations.

Similarly, treatment of aminoaldehyde **1** with aliphatic methyl ketones led to the corresponding 8-substituted pyridotheniopyrazine compounds (Scheme 2). It should be noted that the condensation with unsymmetrical aliphatic ketones gives two different products depending on which α -carbon is used for bond formation. Ring closure under the base-catalyzed condensation of **1** with ethyl methyl ketone or methyl phenethyl ketone was found to occur preferentially at the α -CH₃ carbon, even though the isomeric products have been isolated from the reaction mixture with regioselectivity ratios in the formation of 8-monosubstituted versus 7,8-disubstituted products from 70:30 to 80:20, respectively. The regiochemistry of the Friedländer reaction depends on the experimental conditions. We found that the best results were obtained when ethanolic potassium hydroxide was used. However, other catalysts, including SnCl₂·2H₂O, CeCl₃·7H₂O, HCl, pyrrolidine or piperidine, also promoted the reaction successfully, but the regioselectivity and the yields were lower.



Scheme 2. Preparation of pyridotheniopyrazine derivatives **3m–o** and **4n,o**.

Analogously, the classical Friedländer reaction has been extended and applied to cyclic ketones. Thus, we thought that similar polycyclic compounds containing a fused pyridotheniopyrazine moiety **6a–g** could be afforded by the reaction of **1** with carbocyclic or heterocyclic ketones through this conversion. Indeed, aminoaldehyde **1** reacts with 1-indanone giving rise to adduct **7** in 80% yield (Scheme 3). Consequently, the availability and structural



Scheme 3. Synthesis of pyridotheniopyrazines **6a–g**, **7**, **8a,b**, and pyrimidopyridotheniopyrazines **9a,b**.

variety of cyclic ketones provide an easy and direct access to a number of fused heterocyclic systems for which in many cases alternate annulation methods are not readily available.

With the intent to introduce more diversity in the products employing this strategy, it was decided to carry out the Friedländer reaction with other reactive α -methylene groups. Thus, **1** condenses with acetonitrile to give the 7-amino adduct **8a**, whereas its condensation with malononitrile takes place via intramolecular addition of the amino group to the cyano function on the intermediate produced by initial intermolecular condensation to give the amino-cyano derivative **8b** (**Scheme 3**). Similar condensations with barbituric or 1,3-dimethylbarbituric acids yielded pyrimidothienopyrazines **9a,b**.

All bridging ligands were unambiguously characterized by ^1H NMR, ^{13}C NMR, MS, and elemental analyses. Thus, for example, the ^1H NMR spectra of **3a–o** show two doublets at $\delta=7.20–8.40$ and $8.10–8.50$ ($J=8.5$ Hz) due to the protons of the pyridine skeleton. The pyrazine ring was also distinguished by two doublets at $\delta=8.67–8.78$ and $8.80–8.94$ ($J=2.4$ Hz) due to the H-3 and H-2 protons, respectively. On the other hand, the structural determination of **3a** was unequivocally established by the X-ray structure determination of a monocrystal (**Fig. 2**).



Fig. 2. Crystal X-ray structure of compound **3a** represented by thermal ellipsoids at the 50% level. Hydrogen atoms have been omitted for clarity. The color-labeling scheme is as follows: carbon (gray), nitrogen (blue), and sulfur (yellow).

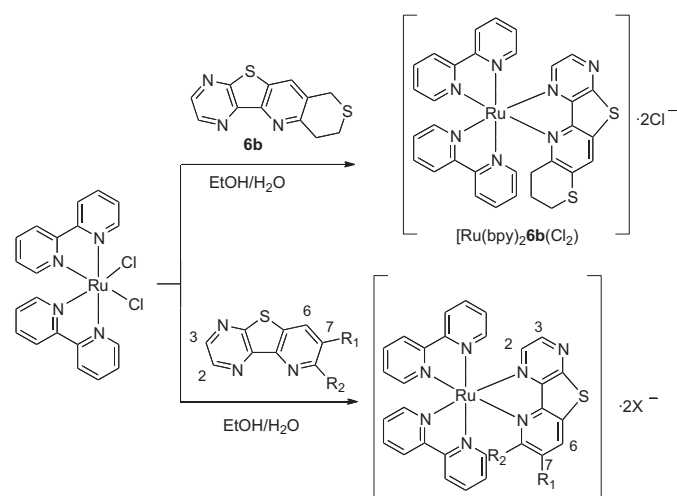
2.2. Electronic spectroscopy

UV-vis absorption spectra of the ligands **3a**, **3c–e**, and **3l** were recorded in acetonitrile at room temperature, and the results are shown in **Table 1**. Quantum yields were also determined. The maximum of the emission band shifts from 412 nm for **3a** to 430 nm for **3c** and 471 nm for **3d**, reflecting a steady progression to lower energy with increasing the delocalization of the system. The pyrene group significantly stabilized the energy of the excited-state by enhancement of conjugation via delocalization of π electrons along the pyrene backbone. Consequently, **3d** showed a huge bathochromic shift of the luminescence compared to **3a** ($\lambda_{\text{max}}=471$ vs 412 nm). The fluorescence quantum yields (Φ_f) for the systems

were determined in acetonitrile at 25 °C upon excitation at the corresponding λ_{max} absorption wavelengths, and the results are given in **Table 1**. The Φ_f values for these systems cover a wide range from **3f**, which only shows a very low quantum yield (0.0080), to **3c** and **3d**, which exhibited higher fluorescence efficiency levels (0.26 and 0.28, respectively). As a result of the more extended π -delocalization, quantum yields remain high even in those compounds exhibiting longer emission wavelengths. It is also worth mentioning that the Stokes shifts of the new ligands vary in the range of 62–160 nm, correlating nicely with the increasing longitudinal organization of the molecule.¹⁵

2.3. Complexation with Ru(II)

Ru(II) was selected as a central ion for studying the complexation ability of our bridged analogues of bipyridine. The Ru(II) complexes were prepared from equimolecular amounts of [Ru(bpy)₂Cl₂] and the appropriate ligand (**L**) in ethanol/water. The resulting dichloride [Ru(bpy)₂**L**]Cl₂ complexes were isolated in acceptable to good yields (61–80%) (**Scheme 4**). For [Ru(bpy)₂**8b**]Cl₂ complex, dichloride salt can be converted into the corresponding organic-soluble hexafluorophosphate with NH₄PF₆.



Ligand	Complex	R ₁	R ₂
3e	[Ru(bpy) ₂ 3e (Cl ₂)]	H	4-pyridyl
3l	[Ru(bpy) ₂ 3l (Cl ₂)]	H	4-nitrophenyl
3m	[Ru(bpy) ₂ 3m (Cl ₂)]	H	CH ₃
8b	[Ru(bpy) ₂ 8b (PF ₆) ₂]	CN	NH ₂

Scheme 4. Synthesis of Ruthenium(II) complexes.

Table 1
Photophysical data for pyridothienopyrazine derivatives **3**

Compd	Absorption ^a λ_{max} [nm] ($\log \epsilon$)	Emission ^b λ_{max} [nm] 298 K	Φ_{EM}^c	Stokes shift
3a	265 (4.04), 319 (4.02)	412	0.09	93
3c	328 (3.30)	430	0.26	102
3d	256 (4.03), 311 (3.99)	471	0.28	160
3f	294 (3.90)	372	0.008	78
3l	313 (310)	375	0.02	62

^a Solvent: CH₃CN (10^{-5} M) at 25 °C.

^b Solvent: CH₃CN (5×10^{-5} M) at 25 °C. The spectra were recorded upon excitation on the long-wavelength absorption maxima.

^c Fluorescence quantum yields (Φ_{EM}) values were determined in acetonitrile solution at 25 °C, using 8,10-diphenyl anthracene as standard ($\Phi_{\text{EM}}=0.95$, in ethanol), by excitation on λ_{max} absorption wavelengths.

Unfortunately, we were not able to grow suitable crystals, but electrospray ionization mass spectrometry (ESI-MS) and NMR spectroscopy were used to elucidate the formation of complexes and their composition. The HRMS-ESI supported the proposed structures showing *m/z* values and isotopic pattern distributions in excellent agreement with the calculated ones (see **Experimental section**). A comparison between the calculated mass distribution pattern for the doubly charged species [Ru(bpy)₂**8b**]⁺² and the experimental data unambiguously confirms the formation of the desired complex. Moreover, the reaction of pyridothienopyrazine (ptp) ligands with [Ru(bpy)₂Cl₂] in ethanol/water produced changes in their ^1H NMR spectra that are consistent with the formation of the corresponding complexes. **Table 2** compares characteristic chemical shifts for H-2, H-3, H-6, and H-7 into the free

Table 2
¹H NMR data ($\Delta\delta$)^a for the Ru(II) complexes

Ligand	Complex	H-2	H-3	H-6	H-7
3e	[Ru(bpy) ₂ 3e]Cl ₂	-0.74	0.11	0.85	-0.37
3l	[Ru(bpy) ₂ 3l]Cl ₂	-0.90	0.20	1.27	-0.05
3m	[Ru(bpy) ₂ 3m]Cl ₂	-0.64	0.33	1.23	0.16
8b	[Ru(bpy) ₂ 8b](PF ₆) ₂	-0.96	0.19	0.70	

^a The δ values are compared to those of the corresponding ligand.

ligands and their corresponding complexes (see Scheme 4 for labeling). The ptp protons are assigned on the basis of their chemical shifts, multiplicity, and an analysis of their 2D-COSY spectra, and the data are summarized in Table 2. The ¹H NMR spectra indicate that upon coordination to Ru the protons at the 3 and 6 positions of the pyridothienopyrazine shift downfield (Table 2 and dotted lines in Fig. 3), which can be attributed to a decreased charge density on the ligand as a consequence of the formation of the Ru–ligand bonds, thereby causing a deshielding effect. Consequently, the H-3 protons of the pyrazine units shifted to larger frequencies (averaged shift: $\Delta\delta=+0.11\text{--}0.33$ ppm), whereas the chemical shifts of the H-6 pyridine protons were strongly affected (averaged shift: $\Delta\delta=+0.70\text{--}1.27$ ppm). Although H-3 is subject to the same effect as H-6, it is less pronounced most likely due to back bonding existence in the charge transfer from metal-to-ligand. This back donation is very important in the spectroscopic properties of Ru(II) complexes and its effects are more pronounced in the proximity of the metal center. On the contrary, the H-2 protons of the complexes are shifted upfield ($\Delta\delta=-0.64$ to 0.96 ppm) from those of the pyridothienopyrazine moiety of the corresponding free ligands (Table 2 and solid line in Fig. 3). The H-2 protons point toward the face of the central pyridine ring of the orthogonal bpy ligand (see Fig. 4), causing it to be shielded and shifted upfield. The effect is largely diminished for the more remote H-3 protons.

The arrangement of the 8-substituents as regarding to the pyridothienopyrazine nucleus depends on the dihedral angle α defined

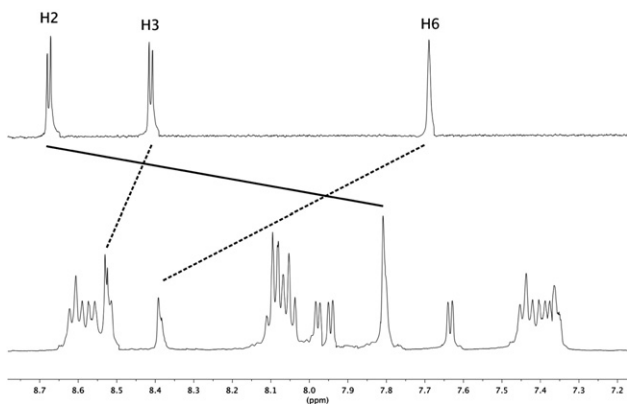


Fig. 3. Partial ¹H NMR spectra (CD₃CN, 298 K, 500 MHz) of ligand **6b** (top) and the [Ru(bpy)₂**6b**]Cl₂ complex (bottom).

Table 3
Photophysical data for ligands **3e**, **3l**, **m**, **6b**, **8b** and their complex derivatives

Ligand	Absorption ^a λ_{\max} [nm] ($\log \epsilon$)	Emission ^b λ_{\max} [nm] 298 K	Φ_{EM}^c	Stokes shift	Complex	Absorption ^a λ_{\max} [nm] ($\log \epsilon$)	Emission ^b λ_{\max} [nm] 298 K	Φ_{EM}^c	Stokes shift
3f	294 (3.90)	372	0.008	78	[Ru(bpy) ₂ 3f]Cl ₂	284 (3.43)	465	0.09	43
3l	313 (3.10)	375	0.02	62	[Ru(bpy) ₂ 3l]Cl ₂	282 (4.77), 425 (4.39)	545	n.d.	120
3m	239 (4.64), 304 (4.47)	380	0.01	76	[Ru(bpy) ₂ 3m]Cl ₂	290 (3.50)	470	0.03	180
6b	252 (5.01), 348 (4.38)	375	0.04	27	[Ru(bpy) ₂ 6b]Cl ₂	284 (4.00), 434 (3.87)	550	0.03	96
8b	251 (4.25), 321 (4.09)	480	0.25	169	[Ru(bpy) ₂ 8b](PF ₆) ₂	285 (4.24), 435 (3.80)	600	0.19	315

^a Solvent: CH₃CN (10⁻⁵ M) at 25 °C.

^b Solvent: CH₃CN (5 × 10⁻⁵ M) at 25 °C. Excitation at the long-wavelength absorption maximum.

^c Fluorescence quantum yields were determined in CH₃CN at 25 °C, using Rhodamine B in ethanol as standard ($\Phi_{EM}=0.65$), at λ_{\max} of absorption wavelengths.

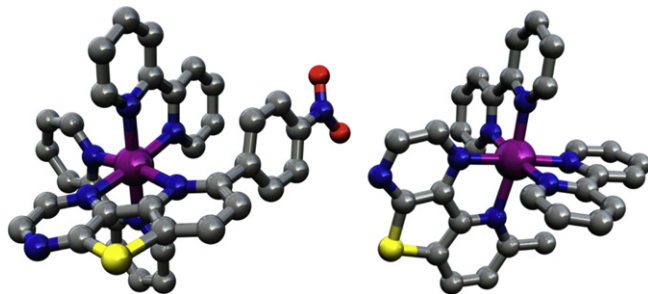


Fig. 4. Calculated structures of [Ru(bpy)₂**3l**]²⁺ (left) and [Ru(bpy)₂**3m**]²⁺ (right) systems.

by the rotation about de 2,2'-bond. For heteroleptic complexes like [Ru(bpy)₂**3e**]Cl₂ or [Ru(bpy)₂**3m**]Cl₂, the substituents tend toward perpendicular orientation, which minimizes the steric hindrance with bipyridine ancillary ligands.¹⁶ This orientation is stabilized by $\pi-\pi$ interactions between the aromatic substituent and one orthogonal pyridine ring, which facilitates interligand communication. Fig. 4 depicts computer simulations for the complexes [Ru(bpy)₂**3l**]Cl₂ and [Ru(bpy)₂**3m**]Cl₂ using the software package Gaussian 03. The structure of [Ru(bpy)₂**3l**]Cl₂ shows a near coplanarity between the *p*-nitrophenyl ring and one bipyridine of the auxiliary ligand. The calculated structure of [Ru(bpy)₂**3m**]Cl₂ displays the proximity of the methyl substituent to a bipyridine ligands, causing the shielding of its protons in the NMR spectra with respect to their position observed for the free ligand ($\Delta\delta=+0.14$ ppm). Thus, the calculated structure for this compound is consistent with spectroscopic data collected.

2.4. Photophysical studies

Since the spectroscopic and electronic properties of metal complexes will depend to a great extent on ligand structure, it was of interest to investigate the absorption and emission properties for these systems. UV-vis spectra were recorded in acetonitrile, and the relevant data are compiled in Table 3. The pyridothienopyrazine nucleus (ptp) may be considered as a 2,2'-bipyridine aza-analogue bridged at the 6 and 6' positions with a single sulfur unit, which is both more delocalized and more electronegative, making it a much better charge acceptor.¹⁷ This difference is evidenced by the absorption maxima observed in the absorption spectra of our free ptps ligands (294–348 nm), when compared to the long-wavelength absorption of bpy at 284 nm.¹⁸ It is noteworthy that the more planar and extensively conjugated is the ptp derivative, the more is shifted the absorption band to lower energies. This is in line with previous studies that showed that when bpy is bridged at the 6 and 6' positions with a single methylene unit, the resulting diazafluorene exhibits a bathochromic shift as would be expected for a more rigid, planar molecule.¹⁷ The absorption graphs for the heteroleptics complexes (Fig. 5) are similar, and the higher energy transitions are observed in the range 280–295 nm, corresponding

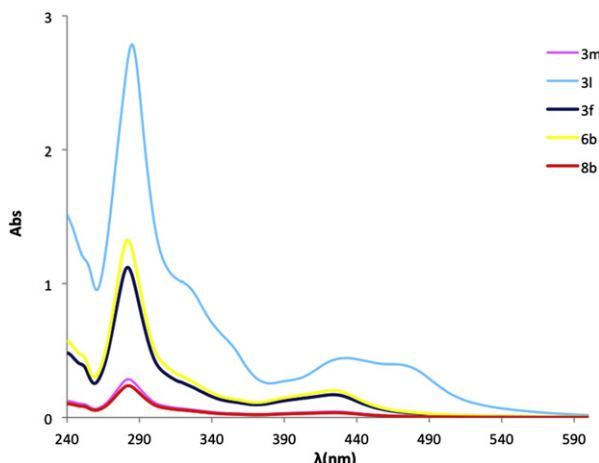


Fig. 5. Absorption graphs for the heteroleptic Ru(II)-complexes measured in 10^{-5} M CH_3CN solutions at room temperature.

to $\pi-\pi^*$ transitions between the aromatic rings of the bipyridine ligands, and transitions between these bipyridines and the ptp nucleus attributed to intraligand $\pi-\pi^*$ transitions by comparison with the spectrum of $[\text{Ru}(\text{bpy})_3]^{2+}$. The visible region of the absorption spectra, at 420–440 nm, is characterized by the presence of medium-intensity absorption bands that can be attributed to metal-to-ligand-charge-transfer (MLCT) transitions. These bands can be attributed to the promotion of an electron from a metal d orbital to a π^* orbital on the most electronegative ligand.^{4a,b} A comparison of these values with the MLCT band observed for $[\text{Ru}(\text{bpy})_3]^{2+}$ ($\lambda_{\max}=452$ nm) shows that for the complexes with ptp derivatives they are observed at shorter wavelengths. This hypsochromic shift is due to ground-state stabilization and destabilization of the excited state because of poor ptp ligand donation, reflecting the influence of the more electronegative pyridothienopyrazine ligand.

The difference in the electronegativity of ptp versus bpy becomes apparent when one examines the emission spectra of $[\text{Ru}(\text{bpy})_2\text{L}]^{2+}$ complexes. Luminescence measurements were recorded in acetonitrile and the relevant data are shown in Table 3 and Fig. 6. For most of the complexes the emission intensity is poor, the spectra showing a long-wavelength component in the range 450–610 nm. When we compared the luminescence properties of $[\text{Ru}(\text{bpy})_3]^{2+}$ ($\lambda_{\max}=620$ nm), the complexes of bridged ptp

derivatives show emission maxima shifted 10–100 nm to a shorter wavelengths, again indicating that the replacement of a bpy ligand by a ptp derivative increases the energy difference between the ground state and the excited charge-transfer state.

In conclusion, a simple method for the preparation of pyridothienopyrazines (ptp) is presented based on the Friedländer condensation of 3-aminothieno[2,3-*b*]pyrazine-2-carbaldehyde with ketones. Using this method, a family of new bidentate bridged ligands for transition metals were prepared and their complexation abilities toward Ruthenium(II) were demonstrated. The photochemical properties of the ligands and their Ruthenium(II) complexes have been also examined. Further studies on this interesting family of ligands are underway and will include variation of the heterodinuclear complexes and the self-assembly of ligand-bridged supramolecular structures.

3. Experimental section

3.1. General

All reagents used were commercial grade chemicals from freshly opened containers. Merck 60 HF₂₅₄₊₃₆₆ foils were used for thin layer chromatography (TLC) and Merck 60 (230–400 mesh) silica gel for flash chromatography. NMR spectra were obtained in a Bruker Avance 500 instrument equipped with a dual cryoprobe for ^1H and ^{13}C or in a Bruker Avance 300 spectrometer. TMS was used as an internal reference. IR spectra were recorded as potassium bromide disks. Mass spectrometry experiments were carried out in a Thermo MAT95XP spectrometer for low resolution EI and FAB using thioglycerol or 3-nitrobenzyl alcohol (3-NBA) as matrix (FAB), or in an LC-Q-q-TOF Applied Biosystems QSTAR Elite spectrometer for low- and high-resolution ESI. Electronic spectra were measured on a Perkin–Elmer Lambda 900 spectrophotometer. Fluorescence spectra were obtained with a Hitachi F-2000 luminescence spectrometer. Melting points were measured using Stuart Scientific SMP3 apparatus and are uncorrected. Microanalyses were performed by the elemental analyses general service of the University of A Coruña.

3.2. Computational methods

Full geometry optimizations of $[\text{Ru}(\text{bpy})_2\text{3l}]^{2+}$ and $[\text{Ru}(\text{bpy})_2\text{3m}]^{2+}$ systems were performed at the HF level by using the Gaussian 03 program package (Revision C.01). In these calculations we used the standard 6-31G basis set for C, H, and N atoms, while for Ru the LanL2DZ valence and effective core potential functions were used. The stationary points found on the potential energy surfaces as a result of the geometry optimizations have been tested to represent energy minima rather than saddle points via frequency analysis.

3.3. Crystallographic material

3a 已在剑桥晶胞数据库中心作为补充出版物编号 CCDC 674102 存储。这些数据可以免费从剑桥晶胞数据库中心通过 www.ccdc.cam.ac.uk/data_request/cif 获得。

3.4. Substituted pyrido[2',3':4,5]thieno[2,3-*b*]pyrazines. General procedure (**3a–o**, **4n,o**, **6a–g**, **7**, **8a,b**, and **9a,b**)

A solution of **1** (0.1 g, 0.55 mmol), a suitable aryl or heteroaryl methyl ketone **2** (0.66 mmol), and a catalytic amount of 10% ethanolic potassium hydroxide in ethanol (10 mL) was refluxed until all starting material had disappeared as checked by TLC (1–24 h). The

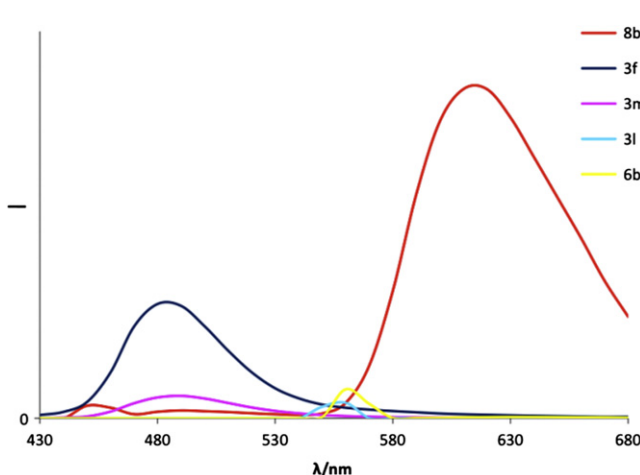


Fig. 6. Emission graphs for the heteroleptic Ru(II)-complexes measured in 5×10^{-5} M CH_3CN solutions at room temperature.

solvent was evaporated, and the resulting residue was recrystallized from ethanol or purified by medium-pressure chromatography on silica gel.

3.4.1. 8-Phenylpyrido[2',3':4,5]thieno[2,3-*b*]pyrazine (3a**).** Recrystallized from ethanol; yield (61%); white solid; mp: 221–225 °C. IR (KBr) 3050, 1738, 1545, 1493, 1451, 1342 cm⁻¹. ¹H NMR (CDCl₃, 300 MHz) δ: 7.47–7.57 (m, 2H, ArH); 8.03 (d, 1H, J=8.5 Hz, H-6); 8.25–8.28 (m, 3H, ArH); 8.32 (d, 1H, J=8.5 Hz, H-7); 8.71 (d, 1H, J=2.4 Hz, H-3); 8.90 (d, 1H, J=2.4 Hz, H-2). ¹³C NMR (CDCl₃, 75 MHz) δ: 120.5, 127.2, 129.0, 131.1, 141.5, 142.1, 152.2. MS (FAB) m/z 264 [(MH)⁺, 20]. Anal. Calcd for C₁₅H₉N₃S: C, 68.42; H, 3.45; N, 15.96. Found: C, 68.11; H, 3.21; N, 15.78.

3.4.2. 8-(Naphthacen-2'-yl)pyrido[2',3':4,5]thieno[2,3-*b*]pyrazine (3b**).** Recrystallized from ethanol; yield (93%); white solid; mp: 186–188 °C. IR (KBr) 3045, 2852, 1652, 1530, 1454, 1402, 1339 cm⁻¹. ¹H NMR (CDCl₃, 300 MHz) δ: 7.43–7.49 (m, 3H, ArH); 7.77–7.97 (m, 4H, ArH); 8.09–8.14 (m, 1H); 8.38 (d, 1H, J=8.5 Hz, H-6); 8.69 (d, 1H, J=2.4 Hz, H-3); 8.85 (d, 1H, J=2.4 Hz, H-2). ¹³C NMR (CDCl₃, 75 MHz) δ: 125.2, 125.3, 125.8, 126.6, 128.2, 129.1, 131.2, 131.3, 132.8, 133.7, 137.7, 142.2, 143.4, 145.1, 147.7, 157.3, 158.2. MS (FAB) m/z 314 [(MH)⁺, 100]. Anal. Calcd for C₁₉H₁₁N₃S: C, 72.82; H, 3.54; N, 13.41. Found: C, 72.36; H, 3.75; N, 13.12.

3.4.3. 8-(Phenanthren-2'-yl)-pyrido[2',3':4,5]thieno[2,3-*b*]pyrazine (3c**).** Recrystallized from CH₂Cl₂/hexane, 6:4; yield (72%); pale yellow solid; mp: 219–220 °C. IR (KBr) 2921, 1714, 1598, 1564, 1178 cm⁻¹. ¹H NMR (CDCl₃, 300 MHz) δ: 7.61–7.73 (m, 2H, ArH); 7.80 (d, 1H, J=8.8 Hz, H-7); 7.90–7.93 (m, 2H, ArH); 8.20 (d, 1H, J=8.5 Hz, H-6); 8.37 (d, 1H, J=8.5 Hz); 8.53–8.55 (m, 1H, ArH); 8.71; 8.73–8.79 (m, 2H, ArH); 8.81 (d, 1H, J=8.0 Hz, ArH); 8.94 (d, 1H, J=2.4 Hz, H-2). ¹³C NMR (CDCl₃, 75 MHz) δ: 121.0, 122.9, 123.3, 125.4, 126.7, 126.9, 127.3, 127.4, 128.6, 130.0, 131.0, 131.9, 132.2, 132.4, 133.0, 136.4, 142.3, 144.5, 145.1, 147.8. MS (FAB) m/z 364 [(MH)⁺, 70]. Anal. Calcd for C₂₃H₁₃N₃S: C, 76.01; H, 3.61; N, 11.56; S, 8.82. Found: C, 76.31; H, 3.56; N, 11.51; S, 8.62.

3.4.4. 6-(Pyren-2'-yl)-pyrido[4',5':4,5]thieno[2,3-*b*]pyrazine (3d**).** Recrystallized from CH₂Cl₂/hexane, 1:1; yield (69%); yellow solid; mp: 262–264 °C. IR (KBr) 3038, 2324, 1789, 1585, 1433, 1328, 1132 cm⁻¹. ¹H NMR (CDCl₃, 300 MHz) δ: 8.00 (d, 1H, J=8.3 Hz, ArH); 8.03 (d, 1H, J=5.6 Hz, ArH); 8.05 (d, 1H, J=7.6 Hz, ArH); 8.09 (d, 1H, J=9.3 Hz, ArH); 8.15 (s, 1H, ArH); 8.22–8.24 (m, 2H, ArH); 8.29 (d, 1H, J=7.9 Hz, H-6); 8.36 (d, 1H, J=7.9 Hz, H-7); 8.41–8.45 (m, 2H, ArH); 8.71 (d, 1H, J=2.4 Hz, H-3); 8.89 (d, 1H, J=2.4 Hz, H-2). ¹³C NMR (CDCl₃, 75 MHz) δ: 124.6, 124.8, 125.5, 126.1, 127.5, 128.1, 128.3, 128.4, 129.0, 131.4, 132.8, 135.1, 142.4, 143.6, 145.2, 148.1, 157.2, 158.7. MS (FAB) m/z 388 [(MH)⁺, 50]. Anal. Calcd for C₂₅H₁₃N₃S: C, 77.50; H, 3.38; N, 10.98; S, 8.28. Found: C, 77.47; H, 3.38; N, 10.67; S, 8.47.

3.4.5. 8-(Pyri-2'-yl)-pyrido[2',3':4,5]thieno[2,3-*b*]pyrazine (3e**).** Recrystallized from CH₂Cl₂; yield (71%); yellow solid; mp: 245–247 °C. IR (KBr) 3089, 3047, 1599, 1341, 1281, 1179 cm⁻¹. ¹H NMR (CD₃CN, 500 MHz) δ: 7.83 (d, 1H, J=8.5 Hz, H-6), 7.96 (d, 1H, J=8.5 Hz, H-7), 8.00–8.05 (m, 4H, Py); 8.43 (d, 1H, J=8.5 Hz, H-3), 8.61 (d, 1H, J=2.4 Hz, H-2). ¹³C NMR (CDCl₃, 125 MHz) δ: 121.4, 121.6, 134.2, 134.7, 143.3, 144.4, 144.9, 145.5, 147.8, 151.0, 152.9, 157.4. MS (FAB) m/z 265 [(MH)⁺, 80]. Anal. Calcd C₁₄H₈N₄S: C, 63.62; H, 3.05; N, 21.20; S, 12.13. Found: C, 63.31; H, 2.90; N, 21.55; S, 12.24.

3.4.6. 8-(Pyrid-4'-yl)-pyrido[2',3':4,5]thieno[2,3-*b*]pyrazine (3f**).** Recrystallized from ethanol; yield (50%); yellow crystals; mp: 233–235 °C. IR (KBr) 3050, 1738, 1545, 1493, 1451, 1342, 1183 cm⁻¹.

¹H NMR (CDCl₃, 300 MHz) δ: 7.36–7.39 (m, 2H, Py), 7.82–7.84 (m, 2H, Py); 8.40 (d, J=9.4 Hz, 1H), 8.64–8.90 (m, 3H). ¹³C NMR (CDCl₃, 75 MHz) δ: 121.3, 121.9, 132.2, 135.4, 139.6, 141.0, 149.5. MS (FAB) m/z 265 [(MH)⁺, 100]. Anal. Calcd C₁₄H₈N₄S: C, 63.62; H, 3.05; N, 21.20. Found: C, 63.39; H, 3.21; N, 21.28.

3.4.7. 8-(Pyrid-3'-yl)-pyrido[2',5':3,5]thieno[2,3-*b*]pyrazine (3g**).** Recrystallized from ethanol; yield (79%); yellow crystals; mp: 230–232 °C. IR (KBr) 3046, 1681, 1483, 1140 cm⁻¹. ¹H NMR (CDCl₃, 300 MHz) δ: 8.03 (d, 1H, J=8.5 Hz, H-6), 8.38 (d, 1H, J=8.5 Hz, H-7), 8.40–8.65 (m, 3H, Py); 8.78 (d, 1H, J=2.4 Hz, H-3); 8.93 (d, 1H, J=2.4 Hz, H-2); 9.18 (s, 1H). ¹³C NMR (CDCl₃, 75 MHz) δ: 120.6, 123.7, 132.3, 133.6, 134.2, 135.1, 142.4, 143.7, 144.8, 148.0, 148.4, 150.3, 153.9, 157.5. MS (FAB) m/z 265 [(MH)⁺, 70]. Anal. Calcd C₁₄H₈N₄S: C, 63.62; H, 3.05; N, 21.20; S, 12.13. Found: C, 63.22; H, 3.12; N, 21.33; S, 12.33.

3.4.8. 8-(Thien-2'-yl)pyrido[2',3':4,5]thieno[2,3-*b*]pyrazine (3h**).** Recrystallized from (CH₂Cl₂); yield (74%); yellow solid; mp: 250–251 °C. IR (KBr) 3047, 1738, 1542, 1480, 1431, 1166 cm⁻¹. ¹H NMR (CDCl₃, 300 MHz) δ: 7.45–7.49 (m, 1H, thienyl); 7.92–7.96 (m, 2H, thienyl); 8.09–8.11 (m, 1H); 8.25 (d, 1H, J=8.5 Hz, H-7); 8.71 (d, 1H, J=2.4 Hz, H-3); 8.92 (d, 1H, J=2.4 Hz, H-2). ¹³C NMR (CDCl₃, 75 MHz) δ: 119.0, 125.5, 128.4, 132.4, 142.1, 143.2, 151.8, 157.5. MS (FAB) m/z 270 [(MH)⁺, 100]. Anal. Calcd C₁₃H₇N₃S₂: C, 57.97; H, 2.62; N, 15.60. Found: C, 57.59; H, 2.99; N, 15.12.

3.4.9. 8-(5'-Bromothien-2'-yl)pyrido[2',3':4,5]thieno[2,3-*b*]pyrazine (3i**).** Recrystallized from (CH₂Cl₂); yield (69%); yellow solid; mp: 253–255 °C. IR (KBr) 3048, 2323, 1569, 1419, 1214 cm⁻¹. ¹H NMR (CDCl₃, 300 MHz) δ: 7.12 (d, 1H, J=3.9 Hz, thienyl); 7.52 (d, 1H, J=3.9 Hz, thienyl); 7.83 (d, 1H, J=8.5 Hz, H-6); 8.25 (d, 1H, J=8.5 Hz, H-7); 8.69 (d, 1H, J=2.4 Hz, H-3); 8.90 (d, 1H, J=2.4 Hz, H-2). ¹³C NMR (CDCl₃, 75 MHz) δ: 116.1, 118.7, 125.7, 131.0, 132.0, 132.7, 142.5, 143.6, 144.7, 145.6, 147.6, 151.0, 157.7. MS (FAB) m/z 348 [(MH)⁺, 95]. Anal. Calcd C₁₃H₆N₃S₂Br: C, 44.84; H, 1.74; N, 12.07; S, 18.42. Found: C, 44.54; H, 1.34; N, 11.68; S, 18.03.

3.4.10. 8-(Furan-2'-yl)pyrido[2',3':4,5]thieno[2,3-*b*]pyrazine (3j**).** Recrystallized from Et₂O/hexane 1:1; yield (88%); pale yellow solid; mp: 184–186 °C. IR (KBr) 2917, 2849, 1595, 1488, 1339, 1176 cm⁻¹. ¹H NMR (CDCl₃, 300 MHz) δ: 6.62–6.65 (m, 1H, furyl); 7.45 (d, 1H, J=3.5 Hz, furyl); 7.61–7.65 (m, 1H, furyl); 7.99 (d, 1H, J=8.5 Hz, H-6); 8.28 (d, 1H, J=8.5 Hz, H-7); 8.70 (d, 1H, J=2.4 Hz, H-3); 8.89 (d, 1H, J=2.4 Hz, H-2). ¹³C NMR (CDCl₃, 75 MHz) δ: 110.0, 112.4, 119.0, 128.7, 131.8, 132.3, 142.2, 143.4, 144.8, 147.4, 148.6, 153.0. MS (FAB) m/z 254 [(MH)⁺, 90]. Anal. Calcd C₁₃H₇N₃OS: C, 61.65; H, 2.79; N, 16.59; S, 12.66. Found: C, 61.42; H, 2.98; N, 16.17; S, 12.20.

3.4.11. 8-(Thiazol-2'-yl)pyrido[2',3':4,5]thieno[2,3-*b*]pyrazine (3k**).** Recrystallized from CH₂Cl₂; yield (58%); yellow solid; mp: 215–217 °C. IR (KBr) 2353, 1567, 1543, 1446, 1326, 1309, 1083 cm⁻¹. ¹H NMR (CDCl₃, 300 MHz) δ: 7.55 (d, 1H, J=2.7 Hz, thiazolyl); 7.96 (d, 1H, J=2.7 Hz, thiazolyl); 8.34 (d, 1H, J=8.5 Hz, H-6); 8.53 (d, 1H, J=8.5 Hz, H-7); 8.70 (d, 1H, J=2.4 Hz, H-3); 8.93 (d, 1H, J=2.4 Hz, H-2). ¹³C NMR (CDCl₃, 75 MHz) δ: 120.0, 122.0, 132.4, 145.1, 142.2, 143.5, 143.9, 151.2. MS (FAB) m/z 271 [(MH)⁺, 90]. Anal. Calcd C₁₂H₆N₄S₂: C, 53.32; H, 2.24; N, 20.73. Found: C, 53.57; H, 2.54; N, 20.86.

3.4.12. 8-(4'-Nitrophenyl)pyrido[2',3':4,5]thieno[2,3-*b*]pyrazine (3l**).** Recrystallized from CH₂Cl₂/hexane 3:7; yield (84%); yellow solid; mp: 289–291 °C. IR (KBr) 3075, 1672, 1601, 1508, 1335, 1093 cm⁻¹. ¹H NMR (CD₃CN, 500 MHz) δ: 7.55 (d, 1H, J=8.5 Hz, H-6); 7.50–7.56 (m, 4H); 7.72 (d, 1H, J=8.5 Hz, H-7); 8.45 (d, 1H,

$J=2.4$ Hz, H-3); 8.66 (d, 1H, $J=2.4$ Hz, H-2). ^{13}C NMR (CDCl_3 , 125 MHz) δ : 121.0, 124.0, 128.2, 132.4, 134.3, 142.5, 143.9, 144.3, 144.7, 148.1, 153.8. MS (FAB) m/z 309 [(MH^+), 95]. Anal. Calcd $\text{C}_{15}\text{H}_8\text{N}_4\text{O}_2\text{S}$: C, 58.43; H, 2.62; N, 18.17; S, 10.40. Found: C, 58.40; H, 2.95; N, 18.52; S, 10.01.

3.4.13. 8-Methylpyrido[2',3':4,5]thieno[2,3-b]pyrazine (3m). Recrystallized from $\text{AcOEt}/\text{hexane}$ 3:7; yield (87%); yellow solid; mp: 176–178 °C. IR (KBr) 3094, 3046, 2918, 2852, 1979, 1635, 1570, 1545, 1343, 1155 cm^{-1} . ^1H NMR (CD_3CN , 500 MHz) δ : 3.11 (s, 3H); 7.36 (d, 1H, $J=8.5$ Hz, H-6); 7.53 (d, 1H, $J=8.5$ Hz, H-7); 8.32 (d, 1H, $J=2.4$ Hz, H-3); 8.54 (d, 1H, $J=2.4$ Hz, H-2). ^{13}C NMR (CDCl_3 , 75 MHz) δ : 24.6, 123.7, 131.2, 131.5, 142.0, 143.1, 144.8, 147.1, 157.1, 157.9. MS (FAB) m/z 202 [(MH^+), 100]. Anal. Calcd $\text{C}_{10}\text{H}_7\text{N}_3\text{S}$: C, 59.68; H, 3.51; N, 20.88; S, 15.93. Found: C, 59.95; H, 3.60; N, 20.81; S, 15.64.

3.4.14. 8-Ethylpyrido[2',3':4,5]thieno[2,3-b]pyrazine (3n). Recrystallized from $\text{AcOEt}/\text{hexane}$ 4:6; yield (44%); yellow solid; mp: 155–157 °C. IR (KBr) 2921, 2852, 1652, 1530, 1454, 1402, 1339, 1184 cm^{-1} . ^1H NMR (CD_3CN , 300 MHz) δ : 1.18 (t, 3H, $J=6.6$ Hz, CH_3); 2.81 (q, 2H, $J=6.6$ Hz, CH_2); 7.36 (d, 1H, $J=8.5$ Hz, H-6); 7.53 (d, 1H, $J=8.5$ Hz, H-7); 8.32 (d, 1H, $J=2.4$ Hz, H-3); 8.80 (d, 1H, $J=2.4$ Hz, H-2). ^{13}C NMR (CDCl_3 , 75 MHz) δ : 23.0, 29.9, 131.4, 132.3, 134.2, 141.8, 142.7, 145.0, 145.1, 156.9, 157.4. MS (FAB) m/z 216 [(MH^+), 100]. Anal. Calcd $\text{C}_{11}\text{H}_9\text{N}_3\text{S}$: C, 61.37; H, 4.21; N, 19.52; S, 14.89. Found: C, 61.62; H, 4.55; N, 19.20; S, 14.63.

3.4.15. 7,8-Dimethylpyrido[2',3':4,5]thieno[2,3-b]pyrazine (4n). Recrystallized from $\text{AcOEt}/\text{hexane}$ 4:6; yield (23%); yellow solid; mp: 280 °C (dec.). IR (KBr) 3156, 1666, 1598, 1337, 1097, 1034 cm^{-1} . ^1H NMR (CDCl_3 , 300 MHz) δ : 2.46 (s, 3H, CH_3); 2.72 (s, 3H, CH_3); 7.93 (s, 1H, H-6); 8.859 (d, 1H, $J=2.4$ Hz, H-3); 8.76 (d, 1H, $J=2.4$ Hz, H-2). ^{13}C NMR (CDCl_3 , 75 MHz) δ : 27.3, 34.3, 140.2, 141.1, 141.2, 141.9, 142.2, 143.5, 144.1. MS (FAB) m/z 216 [(MH^+), 100]. Anal. Calcd $\text{C}_{11}\text{H}_{13}\text{N}_3\text{S}$: C, 61.37; H, 4.21; N, 19.52; S, 14.89. Found: C, 61.21; H, 4.40; N, 19.70; S, 14.69.

3.4.16. 8-(2'-Phenylethyl)pyrido[2',3':4,5]thieno[2,3-b]pyrazine (3o). Recrystallized from CH_2Cl_2 ; yield (45%); yellow solid; mp: 150–152 °C. IR (KBr) 3053, 3028, 2851, 1448, 1345, 1178 cm^{-1} . ^1H NMR (CDCl_3 , 300 MHz) δ : 3.17–3.22 (m, 2H); 3.36–3.41 (m, 2H); 7.20–7.33 (m, 6H); 8.12 (d, 1H, $J=8.4$ Hz, H-7); 8.68 (d, 1H, $J=2.4$ Hz, H-3); 8.87 (d, 1H, $J=2.4$ Hz, H-2). ^{13}C NMR (CDCl_3 , 75 MHz) δ : 36.3, 41.2, 123.5, 126.4, 128.1, 128.5, 131.8, 132.0, 141.2, 142.0, 143.2, 145.0, 147.3, 157.6, 160.9. MS (FAB) m/z 292 [(MH^+), 100]. Anal. Calcd $\text{C}_{17}\text{H}_{13}\text{N}_3\text{S}$: C, 70.08; H, 4.50; N, 14.42; S, 11.00. Found: C, 69.81; H, 4.76; N, 14.57; S, 10.86.

3.4.17. 7-Benzyl-8-methylpyrido[2',3':4,5]thieno[2,3-b]pyrazine (4o). Recrystallized from CH_2Cl_2 ; yield (11%); pale yellow solid; mp: 162–164 °C. NMR (CDCl_3 , 300 MHz) δ : 2.77 (s, 3H); 4.18 (s, 2H); 7.17–7.19 (m, 2H); 7.19–7.35 (m, 3H); 7.85 (s, 1H); 8.62 (d, 1H, $J=2.4$ Hz, H-3); 8.80 (d, 1H, $J=2.4$ Hz, H-2). ^{13}C NMR (CDCl_3 , 75 MHz) δ : 36.3, 40.2, 123.5, 126.0, 128.3, 128.5, 131.3, 132.0, 141.2, 142.0, 143.2, 144.9, 147.3, 157.2. MS (FAB) m/z 292 [(MH^+), 60]. Anal. Calcd $\text{C}_{17}\text{H}_{13}\text{N}_3\text{S}$: C, 70.08; H, 4.50; N, 14.42; S, 11.00. Found: C, 69.84; H, 4.65; N, 14.21; S, 11.20.

3.4.18. 6,7-Dihydro-(9H)-pyran[3",4":5',6']pyrido[2',3':4,5]thieno[2,3-c]pyrazine (6a). Recrystallized from $\text{AcOEt}/\text{hexane}$ 2:8; yield (77%); yellow crystals; mp: 218–220 °C. IR (KBr) 3132, 1704, 1615, 1423, 1367, 1306, 898 cm^{-1} . ^1H NMR (CDCl_3 , 300 MHz) δ : 3.52 (t, 2H, $J=6.3$ Hz); 3.90 (t, 2H, $J=6.3$ Hz); 4.26 (s, 2H); 8.11 (s, 1H); 8.68 (d, 1H, $J=2.4$ Hz); 8.84 (d, 1H, $J=2.4$ Hz). ^{13}C NMR (CDCl_3 , 75 MHz) δ :

27.8, 30.9, 33.8, 136.1, 137.9, 138.6, 145.9, 148.9, 149.6, 150.8, 161.4, 162.0. MS (FAB) m/z 244 [(MH^+), 100]. Anal. Calcd $\text{C}_{12}\text{H}_9\text{N}_3\text{OS}$: C, 59.24; H, 3.73; N, 17.27; S, 13.18. Found: C, 59.51; H, 3.87; N, 17.70; S, 13.53.

3.4.19. 6,7-Dihydro-(9H)-thiopyran[3",4":5',6']pyrido[2',3':4,5]thieno[2,3-c]pyrazine (6b). Recrystallized from $\text{AcOEt}/\text{hexane}$ 4:6; yield (79%); yellow solid; mp: 204–206 °C. IR (KBr) 3178, 1713, 1648, 1621, 1428, 1345, 1262, 1076 cm^{-1} . ^1H NMR (CDCl_3 , 300 MHz) δ : 3.10 (t, 2H, $J=6.5$ Hz); 3.51 (t, 2H, $J=6.5$ Hz); 3.96 (s, 2H); 7.98 (s, 1H); 8.65 (d, 1H, $J=2.4$ Hz); 8.82 (d, 1H, $J=2.4$ Hz). ^{13}C NMR (CDCl_3 , 75 MHz) δ : 26.4, 30.1, 33.8, 129.7, 131.6, 132.2, 142.0, 143.1, 144.7, 145.9, 156.5, 157.1. MS (FAB) m/z 260 [(MH^+), 40]. Anal. Calcd $\text{C}_{12}\text{H}_9\text{N}_3\text{S}_2$: C, 55.57; H, 3.50; N, 16.20; S, 24.73. Found: C, 55.25; H, 3.19; N, 16.65; S, 24.91.

3.4.20. 8-Benzoyl-6,7,8,9-tetrahydropyrazine[4',3':4,5]thieno[2,3-b][1,6]naphthyridine (6c). Recrystallized from $\text{AcOEt}/\text{hexane}$ 4:6; yield (82%); yellow solid; mp: 211–213 °C. IR (KBr) 2934, 2817, 1668, 1597, 1432, 1081 cm^{-1} . ^1H NMR (CDCl_3 , 300 MHz) δ : 2.91 (t, 2H, $J=5.9$ Hz); 3.16 (t, 2H, $J=5.9$ Hz); 3.76 (s, 2H); 3.80 (s, 2H); 7.36–7.40 (m, 5H); 8.33 (s, 1H); 8.78 (d, 1H, $J=2.4$ Hz); 8.89 (d, 1H, $J=2.4$ Hz). ^{13}C NMR (CDCl_3 , 75 MHz) δ : 31.4, 49.1, 54.1, 60.4, 126.2, 127.4, 127.9, 128.7, 130.6, 137.5, 140.5, 141.4, 142.5, 143.1, 144.7, 153.9, 155.8. MS (FAB) m/z 333 [(MH^+), 100]. Anal. Calcd $\text{C}_{19}\text{H}_{16}\text{N}_4\text{S}$: C, 68.65; H, 4.85; N, 16.85; S, 9.65. Found: C, 68.48; H, 4.75; N, 16.75; S, 10.02.

3.4.21. 8-Acetyl-6,7,8,9-tetrahydropyrazine[4',3':4,5]thieno[2,3-b][1,6]naphthyridine (6d). Recrystallized from $\text{AcOEt}/\text{hexane}$ 6:4; yield (76%); yellow solid; mp: 234–236 °C. IR (KBr) 2922, 2878, 1752, 1656, 1544, 1321, 1147 cm^{-1} . ^1H NMR (CDCl_3 , 300 MHz) δ : 2.01 (s, 3H); 3.42–3.71 (m, 4H); 3.93 (s, 3H); 7.93 (s, 1H); 8.71 (d, 1H, $J=2.4$ Hz); 8.77 (d, 1H, $J=2.4$ Hz). MS (FAB) m/z 285 [(MH^+), 100]. Anal. Calcd $\text{C}_{14}\text{H}_{12}\text{N}_4\text{OS}$: C, 59.14; H, 4.25; N, 19.70; S, 11.28. Found: C, 59.69; H, 4.44; N, 19.93; S, 11.53.

3.4.22. 7,8-Dihydro-(6H)-cyclopenta[1",2":5',6']pyrido[2',3':4,5]thieno[2,3-b]pyrazine (6e). Recrystallized from $\text{AcOEt}/\text{hexane}$ 1:1; yield (71%); pale yellow solid; mp: 189–191 °C. IR (KBr) 3043, 2951, 1572, 1531, 1432, 1341, 1174, 1032 cm^{-1} . ^1H NMR (CDCl_3 , 300 MHz) δ : 2.26 (q, 2H, $J=7.6$ Hz); 3.12 (t, 2H, $J=7.6$ Hz); 3.24 (t, 2H, $J=7.6$ Hz); 8.01 (s, 1H); 8.61 (d, 1H, $J=2.4$ Hz); 8.79 (d, 1H, $J=2.4$ Hz). ^{13}C NMR (CDCl_3 , 75 MHz) δ : 23.2, 31.1, 34.0, 123.8, 126.6, 131.3, 138.7, 141.9, 142.2, 142.6, 143.2, 166.2. MS (FAB) m/z 228 [(MH^+), 90], 202 (15). Anal. Calcd $\text{C}_{12}\text{H}_9\text{N}_3\text{S}$: C, 63.41; H, 3.99; N, 18.49; S, 14.11. Found: C, 63.22; H, 4.08; N, 18.34; S, 14.36.

3.4.23. 6,7,8,9-Tetrahydropyrido[4',3':4,5]thieno[3,2-b]quinoline (6f). Recrystallized from $\text{AcOEt}/\text{hexane}$ 3:7; yield (73%); pale yellow solid; mp: 170–172 °C. IR (KBr) 3040, 2938, 1528, 1394, 1204, 1154, 1084 cm^{-1} . ^1H NMR (CDCl_3 , 300 MHz) δ : 1.75–2.04 (m, 4H); 3.01 (t, 2H, $J=6.5$ Hz); 3.22 (t, 2H, $J=6.5$ Hz); 7.90 (s, 1H); 8.61 (d, 1H, $J=2.4$ Hz); 8.78 (d, 1H, $J=2.4$ Hz). ^{13}C NMR (CDCl_3 , 75 MHz) δ : 22.5, 22.9, 29.7, 32.8, 131.1, 131.7, 133.8, 141.7, 142.7, 145.1, 145.2, 157.0, 157.6. MS (FAB) m/z 242 [(MH^+), 100]. Anal. Calcd $\text{C}_{13}\text{H}_{11}\text{N}_3\text{S}$: C, 64.70; H, 4.59; N, 17.41; S, 13.29. Found: C, 64.45; H, 4.54; N, 17.43; S, 13.58.

3.4.24. 7,8,9,10-Tetrahydro-(6H)-cyclohepta[1",2":5',6']pyrido[2',3':4,5]thieno[2,3-b]pyrazine (6g). Recrystallized from $\text{AcOEt}/\text{hexane}$ 1:1; yield (71%); yellow solid; mp: 148–150 °C. IR (KBr) 2921, 2851, 1650, 1399, 1141 cm^{-1} . ^1H NMR (CDCl_3 , 300 MHz) δ : 1.73–1.90 (m, 6H); 2.92–2.97 (m, 2H); 3.27–3.33 (m, 2H); 7.90 (s, 1H); 8.58 (d, 1H, $J=2.4$ Hz); 8.76 (d, 1H, $J=2.4$ Hz). ^{13}C NMR (CDCl_3 , 75 MHz) δ : 26.6, 28.1, 32.2, 35.9, 39.3, 130.7, 132.3, 139.6, 141.8,

142.5, 144.5, 145.8, 156.8, 163.3. MS (FAB) m/z 256 [(MH $^+$), 90]. Anal. Calcd C₁₄H₁₃N₃S: C, 65.85; H, 5.13; N, 16.46; S, 12.56. Found: C, 65.79; H, 5.39; N, 16.42; S, 12.40.

3.4.25. 6H-Indene[1'',2'':5',6']pyrido[2',3':4,5]thieno[2,3-b]pyrazine (7). Recrystallized ethanol/acetone; yield (80%); yellow crystals; mp: 240–242 °C. IR (KBr) 3190, 2919, 2851, 1666, 1573, 1548, 1513, 1244 cm $^{-1}$. 1 H NMR (CDCl₃, 300 MHz) δ : 4.07 (s, 1H); 7.74–7.77 (m, 5H); 8.22 (s, 1H); 8.62 (d, 1H, J =2.4 Hz); 8.70 (d, 1H, J =2.4 Hz). 13 C NMR (CDCl₃, 75 MHz) δ : 31.0, 108.9, 122.5, 123.6, 125.8, 126.7, 127.4, 129.8, 133.3, 137.7, 140.7, 140.8, 142.1, 142.5, 148.2, 155.0. MS (FAB) m/z 276 [(MH $^+$), 100]. Anal. Calcd C₁₆H₉N₃S: C, 69.80; H, 3.29; N, 15.26; S, 11.65. Found: C, 69.47; H, 3.56; N, 15.67; S, 11.30.

3.4.26. 8-Aminopyrido[2',3':4,5]thieno[2,3-b]pyrazine (8a). Recrystallized from AcOEt/hexane 3:7; yield (77%); yellow crystals; mp: 256–258 °C. IR (KBr) 3460, 3340, 2920, 2851, 1731, 1621, 1519, 1186 cm $^{-1}$. 1 H NMR (CDCl₃, 300 MHz) δ : 4.88 (s, 2H); 6.84 (d, 1H, J =8.5 Hz, H-7); 7.98 (d, 1H, J =8.5 Hz, H-6); 8.62 (d, 1H, J =2.4 Hz, H-3); 8.77 (d, 1H, J =2.4 Hz, H-2). 13 C NMR (CDCl₃, 75 MHz) δ : 111.5, 128.8, 130.9, 132.2, 132.9, 133.5, 141.7, 141.8, 142.7. MS (FAB) m/z 203 [(MH $^+$), 40]. Anal. Calcd C₉H₆N₄S: C, 53.45; H, 2.99; N, 27.70; S, 15.86. Found: C, 53.81; H, 2.84; N, 27.65; S, 15.70.

3.4.27. 8-Amino-7-cyanopyrido[2',3':4,5]thieno[2,3-b]pyrazine (8b). Recrystallized from ethanol; yield (89%); yellow crystals; mp: >300 °C. IR (KBr) 3489, 3139, 2216, 1633, 1580, 1344, 1190, 974 cm $^{-1}$. 1 H NMR (CDCl₃, 300 MHz) δ : 6.93 (s, 2H); 7.76 (s, 1H, H-6); 8.32 (d, 1H, J =2.4 Hz, H-3); 8.70 (d, 1H, J =2.4 Hz, H-2). 13 C NMR (CDCl₃, 75 MHz) δ : 92.2, 116.5, 120.2, 139.0, 142.7, 142.8, 143.7, 144.5, 149.7, 158.4. MS (FAB) m/z 228 [(MH $^+$), 50]. Anal. Calcd C₁₀H₅N₅S: C, 52.85; H, 2.22; N, 30.82; S, 14.11. Found: C, 52.66; H, 2.41; N, 30.68; S, 14.35.

3.4.28. 2,4-Dioxo-1,2,3,4-tetrahydropyrimido[2'',3'':5',6']pyrido[2',3':4,5]thieno[2,3-b]pyrazine (9a). Recrystallized from AcOEt; yield (70%); yellow solid; mp: >300 °C. IR (KBr) 3115, 2917, 2819, 1667, 1613, 1562, 1266, 1093 cm $^{-1}$. 1 H NMR (CDCl₃, 300 MHz) δ : 6.71 (s, 1H); 7.55 (s, 1H); 8.37 (s, 1H); 8.73 (d, 1H, J =2.4 Hz); 8.85 (d, 1H, J =2.4 Hz). 13 C NMR (CDCl₃, 75 MHz) δ : 56.5, 79.4, 114.9, 123.0, 136.6, 142.6, 143.5, 143.6, 144.1, 144.2, 146.1, 157.4, 158.0. MS (ESI) m/z 271. Anal. Calcd C₁₁H₅N₅O₂S: C, 48.71; H, 1.86; N, 25.85; S, 11.82. Found: C, 48.59; H, 1.97; N, 25.79; S, 11.57.

3.4.29. 1,3-Dimethyl-2,4-dioxo-1,2,3,4-tetrahydropyrimido[2'',3'':5',6']pyrido[2',3':4,5]thieno[2,3-b]pyrazine (9b). Recrystallized from ethanol; yield (76%); yellow crystals; mp: 291–293 °C. IR (KBr) 3178, 1713, 1648, 1428, 1345, 1076 cm $^{-1}$. 1 H NMR (CDCl₃, 300 MHz) δ : 2.89 (s, 3H); 3.08 (s, 3H); 8.41 (d, 1H, J =2.4 Hz); 8.47 (d, 1H, J =2.4 Hz); 8.87 (s, 1H). 13 C NMR (CDCl₃, 75 MHz) δ : 27.2, 28.3, 118.8, 123.6, 138.9, 143.5, 143.8, 147.2, 151.2, 152.4, 154.8, 155.7. MS (FAB) m/z 300 [(MH $^+$), 100]. Anal. Calcd C₁₃H₉N₅O₂S: C, 52.17; H, 3.03; N, 23.40; S, 10.71. Found: C, 52.64; H, 3.41; N, 23.22; S, 10.41.

3.5. Preparation of Ru(II) complexes

To prepare the Ru(II) complexes, a mixture of [Ru(bpy)₂Cl₂] (200 mg, 1.11 mmol) and the appropriate ligand (**3e**, **3l**, **3m**, **6b** or **8b**) (1.11 mmol), in ethanol/water (1:3) (15 mL), was heated under reflux in an inert atmosphere of argon until all starting materials had disappeared as checked by TLC. The suspension was concentrated in vacuo and the residue was purified by column chromatography on silica gel.

3.5.1. [Ru(bpy)₂3e**]Cl₂.** Acetone/H₂O (1:1) as eluent; yield (61%); black solid. 1 H NMR (D₂O, 500 MHz) δ : 6.94 (t, 1H, J =6.9 Hz), 7.23 (t,

1H, J =6.2 Hz), 7.32 (m, 2H), 7.43 (t, 1H, J =6.2 Hz), 7.45 (t, 1H, J =6.9 Hz), 7.59 (d, 1H, J =8.5 Hz, H-7), 7.70 (t, 1H, J =7.9 Hz), 7.84–7.86 (m, 1H), 7.87 (t, 1H, J =3.0 Hz, H-2), 7.94 (t, 1H, J =7.8 Hz), 8.05–8.13 (m, 5H), 8.19 (d, 1H, J =5.4 Hz), 8.38 (d, 2H, J =7.8 Hz), 8.45–8.47 (m, 3H), 8.54 (d, 1H, J =3.0 Hz, H-3), 8.68 (d, 1H, J =8.5 Hz, H-6). 13 C NMR (D₂O, 125 MHz) δ : 123.2, 123.6, 124.1, 124.4, 126.9, 127.1, 127.2, 127.4, 127.8, 128.5, 133.8, 134.4, 135.1, 137.5, 138.4, 138.5, 138.6, 139.2, 144.3, 145.1, 146.1, 148.7, 149.1, 150.8, 152.1, 152.4, 153.0, 153.7, 153.9, 157.0, 157.1, 157.8, 161.3. HRMS-ESI (m/z) calcd for [M–Cl $^-$] $^{+}$ 713.0571, found 713.0536; calcd for [M–2Cl $^-$] $^{+}$ 339.0438, found 339.0450. Anal. Calcd C₃₄H₂₄Cl₂N₈RuS: C, 54.55; H, 3.23; N, 14.97; S, 4.28. Found: C, 54.01; H, 3.41; N, 15.10; S, 4.67.

3.5.2. [Ru(bpy)₂3l**]Cl₂.** Acetone/H₂O (1:1) as eluent; yield (65%); black solid. 1 H NMR (CD₃CN, 500 MHz) δ : 6.91 (t, 1H, J =6.9 Hz), 7.22 (d, 1H, J =5.7 Hz), 7.31–7.35 (m, 2H), 7.41–7.48 (m, 1H), 7.50–7.57 (m, 3H), 7.67 (d, 1H, J =8.5 Hz, H-7), 7.76–7.81 (m, 2H+H-2), 7.94–8.02 (m, 2H), 8.11–8.17 (m, 3H), 8.26 (m, 1H, J =5.7 Hz), 8.43–8.53 (m, 4H), 8.65 (d, 1H, J =3.0 Hz, H-3), 8.82 (d, 1H, J =8.5 Hz). 13 C NMR (CD₃CN, 125 MHz) δ : 123.4, 123.8, 126.8, 127.0, 127.5, 127.6, 127.7, 128.2, 128.3, 133.6, 136.8, 138.5, 142.6, 144.9, 148.1, 148.5, 150.9, 151.1, 152.5, 153.2, 154.1, 155.1, 156.8, 156.9, 157.1, 158.1, 162.3. HRMS-ESI (m/z) calcd for [M–2Cl $^-$] $^{+}$ 361.0387, found 361.0394. Anal. Calcd C₃₅H₂₄Cl₂N₈O₂RuS: C, 53.03; H, 3.05; N, 14.14; S, 4.05. Found: C, 52.87; H, 3.01; N, 14.35; S, 3.88.

3.5.3. [Ru(bpy)₂3m**]Cl₂.** Acetone/CH₃CN/H₂O (8:1:1) as eluent; yield (60%); black solid. 1 H NMR (CD₃CN, 500 MHz) δ : 2.76 (s, 3H), 7.40–7.49 (m, 4H), 7.60 (d, 1H, J =6.9 Hz), 7.69 (d, 1H, J =8.5 Hz, H-7), 7.80 (d, 1H, J =5.6 Hz), 7.90 (t, 1H, J =3.0 Hz, H-2), 8.06–8.16 (m, 6H), 8.59 (d, 1H, J =8.5 Hz, H-6), 8.65 (d, 1H, J =3.0 Hz, H-3), 8.67–8.70 (m, 4H). 13 C NMR (CD₃CN, 125 MHz) δ : 21.7, 124.6, 124.7, 127.6, 127.7, 128.1, 128.2, 131.5, 134.2, 138.2, 138.3, 138.5, 144.0, 146.6, 148.8, 150.8, 152.5, 152.6, 152.8, 154.1, 157.1, 157.6, 158.2, 164.0. HRMS-ESI (m/z) calcd for [M–2Cl $^-$] $^{+}$ 307.5389, found 307.5396. Anal. Calcd C₃₀H₂₃Cl₂N₇RuS: C, 52.56; H, 3.38; N, 14.30; S, 4.68. Found: C, 52.79; H, 3.15; N, 14.99; S, 4.37.

3.5.4. [Ru(bpy)₂6b**]Cl₂.** Acetone/H₂O (1:1) as eluent; yield (69%); black solid. 1 H NMR (D₂O, 500 MHz) δ : 2.32–2.36 (m, 2H), 2.60–2.67 (m, 4H), 3.72 (d, 1H, J =16.0 Hz), 3.91 (d, 1H, J =16.0 Hz), 7.25–7.32 (m, 4H), 7.64 (d, 1H, J =6.4 Hz), 7.74 (d, 1H, J =5.9 Hz), 7.88 (d, 1H, J =5.9 Hz), 7.91–8.00 (m, 5H), 8.28 (s, 1H), 8.32 (d, 1H, J =3.0 Hz), 8.41–8.50 (m, 4H). 13 C NMR (D₂O, 125 MHz) δ : 25.4, 30.2, 31.0, 124.2, 124.3, 127.2, 127.5, 131.4, 132.7, 135.6, 138.1, 138.2, 138.4, 143.6, 145.3, 149.2, 151.8, 152.2, 152.5, 153.1, 153.4, 157.0, 157.1, 157.2, 158.1, 162.1. HRMS-ESI (m/z) calcd for [M–2Cl $^-$] $^{+}$ 336.5322, found 336.5338. Anal. Calcd C₃₂H₂₅Cl₂N₇RuS: C, 51.68; H, 3.39; N, 13.18; S, 8.62. Found: C, 51.90; H, 3.12; N, 13.73; S, 8.91.

3.5.5. [Ru(bpy)₂8b**](PF₆)₂.** Acetone as eluent; yield (79%); black solid. 1 H NMR (CD₃CN, 500 MHz) δ : 5.00 (s, 2H), 7.40–7.54 (m, 3H), 7.65–7.68 (m, 2H), 7.74 (d, 1H, J =3.0 Hz), 7.85–7.94 (m, 2H), 8.09–8.16 (m, 4H), 8.43–8.37 (m, 1H), 8.48–8.61 (m, 5H), 8.66 (s, 1H). 13 C NMR (CD₃CN, 125 MHz) δ : 124.3, 124.5, 124.9, 127.7, 128.0, 128.4, 134.4, 138.4, 138.5, 139.9, 140.3, 144.1, 144.7, 146.5, 147.4, 152.6, 152.7, 152.9, 154.5, 154.6. HRMS-ESI (m/z) calcd for [M–2PF₆] $^{+}$ 320.5336, found 320.5336. Anal. Calcd C₃₀H₂₁F₁₂N₉P₂RuS: C, 37.27; H, 3.02; N, 15.94; S, 3.42. Found: C, 37.47; H, 2.88; N, 15.76; S, 3.12.

Acknowledgements

The authors are indebted to Centro de Computación de Galicia for providing the computer facilities. This research was supported by Xunta de Galicia (PGIDIT06PXIB103224PR), Ministerio de Educación

y Cultura of Spain, and FEDER (CTQ2007-63839/BQU). A.F.-M. acknowledges a predoctoral fellowship from Xunta de Galicia.

Supplementary data

Supplementary data associated with this article can be found in the online version at doi:10.1016/j.tet.2011.01.066.

References and notes

1. (a) Pitt, W. R.; Parry, D. R.; Perry, B. G.; Groom, C. R. *J. Med. Chem.* **2009**, *52*, 2952; (b) Shinar, J.; Shinar, R. *J. Phys. D: Appl. Phys.* **2008**, *41*, 133001; (c) Sop, F.; Shi, J. *Opt. Sci. Eng.* **2008**, *133*, 351; (d) Wong, T. K. S. In *Handbook of Organics Electronics and Photonics*; Nalwa, H. S., Ed.; American Scientific: Stevenson Ranch, CA, 2008; Vol. 2, pp 413–472.
2. (a) Pluth, M. D.; Bergman, R. G.; Raymond, K. N. *Science* **2007**, *316*, 85; (b) Yoshizawa, M.; Tamura, M.; Fujita, M. *Science* **2006**, *312*, 251; (c) Fujita, M.; Tominaga, M.; Hori, A.; Therrien, B. *Acc. Chem. Res.* **2005**, *38*, 369; (d) Steel, P. J. *Acc. Chem. Res.* **2005**, *38*, 243; (e) Collin, J.-P.; Heitz, V.; Bonnet, S.; Sauvage, J.-P. *Inorg. Chem. Commun.* **2005**, *8*, 1063; (f) Yeh, R. M.; Davis, A. V.; Raymond, K. N. *Supramolecular Systems: Self-Assembly* In: *Comprehensive Coordination Chemistry II*; Fujita, M., Powell, A., Creutz, C. A., Eds.; Pergamon: Oxford, UK, 2004; Vol. 7; p 327; (g) Swiegers, G. F.; Malefeste, T. *Chem. Rev.* **2000**, *100*, 3483.
3. Haslam, E. *Shikimic Acid Metabolism and Metabolites*; John Wiley: New York, NY, 1993.
4. (a) Hung, C.-Y.; Wang, T.-L.; Yang, Y.; Kim, W. Y.; Schmehl, R. H.; Thummel, R. P. *Inorg. Chem.* **1996**, *35*, 5953; (b) Kalyanasundaram, K. *Photochemistry of Poly-pyridine and Porphyrin Complexes*; Academia: San Diego, CA, 1992; (c) Juris, A.; Balzani, V.; Barigelletti, F.; Campagna, S.; Belser, P.; von Zelewsky, A. *Coord. Chem. Rev.* **1988**, *84*, 85.
5. Fallahpour, R.-A. *Synthesis* **2003**, 155.
6. For recent examples, see: (a) Harbuzaru, B. V.; Corma, A.; Rey, F.; Atienzar, P.; Jordá, J. L.; García, H.; Ananás, D.; Carlos, L. D.; Rocha, J. *Angew. Chem., Int. Ed.* **2008**, *47*, 1080; (b) Hovinen, J.; Guy, P. M. *Bioconjugate Chem.* **2009**, *20*, 404; (c) Kido, J. *Chem. Rev.* **2002**, *102*, 2357; (d) Chauvin, A.-S.; Comby, S.; Song, B.; Vandevyver, C. D. B.; Bünzli, J.-C. *G. Chem.—Eur. J.* **2008**, *14*, 1726; (e) Hu, Y.-Zh.; Zhang, G.; Thummel, R. P. *Org. Lett.* **2003**, *5*, 2251.
7. Anthony, J. E. *Chem. Rev.* **2006**, *106*, 5028.
8. (a) Du, C.; Guo, Y.; Liu, Y.; Qiu, W.; Zhang, H.; Gao, X.; Liu, Y.; Qi, T.; Lu, K.; Yu, G. *Chem. Mater.* **2008**, *20*, 4188; (b) Ma, Y.; Sun, Y.; Liu, Y.; Gao, J.; Chen, S.; Sun, X.; Qiu, W.; Yu, G.; Cui, G.; Hu, W.; Zhu, D. *J. Mater. Chem.* **2005**, *15*, 4894; (c) Qi, T.; Guo, Y.; Liu, Y.; Xi, H.; Zhang, H.; Gao, X.; Liu, Y.; Lu, K.; Du, C.; Yu, G.; Zhu, D. *Chem. Commun.* **2008**, 6227.
9. Fernández-Mato, A.; Blanco, G.; Quintela, J. M.; Peinador, C. *Tetrahedron* **2008**, *64*, 3446.
10. (a) Blanco, G.; Fernández-Mato, A.; Quintela, J. M.; Peinador, C. *Synthesis* **2009**, *438*; (b) Blanco, G.; Fernández-Mato, A.; Quintela, J. M.; Peinador, C. *Tetrahedron* **2008**, *64*, 11136; (c) Blanco, G.; Quintela, J. M.; Peinador, C. *Synthesis* **2008**, 1397; (d) Blanco, G.; Quintela, J. M.; Peinador, C. *Tetrahedron* **2008**, *64*, 1333; (e) Alvarez-Sarandes, R.; Peinador, C.; Quintela, J. M. *Tetrahedron* **2001**, *57*, 5413.
11. (a) Chas, M.; Abella, D.; Blanco, V.; Pià, E.; Blanco, G.; Fernández-Mato, A.; Peinador, C.; Quintela, J. M. *J. Am. Chem. Soc.* **2007**, *129*, 13978; (b) Chas, M.; Abella, D.; Blanco, V.; Pià, E.; Platas-Iglesias, C.; Peinador, C.; Quintela, J. M. *Chem.—Eur. J.* **2007**, *13*, 8572; (c) Chas, M.; Platas-Iglesias, C.; Quintela, J. M.; Peinador, C. *Tetrahedron Lett.* **2006**, *47*, 3119; (d) Blanco, V.; Gutiérrez, A.; Platas-Iglesias, C.; Peinador, C.; Quintela, J. M. *J. Org. Chem.* **2009**, *74*, 6577.
12. (a) Friedländer, P. *Ber. Dtsch. Chem. Ges.* **1882**, *15*, 2572; (b) Cheng, C.-C.; Yan, S.-J. *Org. React.* **1982**, *28*, 37.
13. For specialized books, volumes, reviews, and accounts in the Friedländer reaction, see: (a) Marco-Contelles, J.; Pérez Mayoral, E.; Samadi, A.; Carreiras, M. C.; Soriano, E. *Chem. Rev.* **2009**, *109*, 2652; (b) Thummel, R. P. *Synlett* **1992**, *1*; (c) Caluwe, P. *Tetrahedron* **1980**, *36*, 2359; (d) Pflium, D. Friedländer Quinoline Synthesis In *Name Reactions in Heterocyclic Chemistry*; Li, J. J., Corey, E. J., Eds.; Wiley: Hoboken, NJ, 2005; p 411; (e) Balasubramanian, M.; Keay, J. G. In *Comprehensive Heterocyclic Chemistry II*; Katritzky, A. R., Rees, C. W., Scriven, E. F. V., Eds.; Pergamon: New York, NY, 1996; Vol. 5, Chapter 5.06, p 245; Hassner, A.; Stumer, C. *Organic Syntheses Based in Name Reactions*; Pergamon: London, 2002.
14. (a) Blanco, G.; Quintela, J. M.; Peinador, C. *Tetrahedron* **2007**, *63*, 2034; (b) Blanco, G.; Seguí, N.; Quintela, J. M.; Peinador, C.; Chas, M.; Toba, R. *Tetrahedron* **2006**, *62*, 11124.
15. (a) Chouai, L.; Wu, F.; Jang, W.; Thummel, R. P. *Eur. J. Inorg. Chem.* **2003**, 2774; (b) Baba, A. I.; Ensley, H. E.; Schmehl, R. H. *Inorg. Chem.* **1995**, *34*, 1198; (c) Yonemoto, E. H.; Saupe, G. B.; Schmehl, R.; Mallouk, T. E. *J. Am. Chem. Soc.* **1994**, *116*, 4796.
16. Wu, F. Y.; Riesgo, E.; Pavlova, A.; Kipp, R. A.; Schmehl, R. H.; Thummel, R. P. *Inorg. Chem.* **1999**, *38*, 5620.
17. Thummel, R. P.; Declotire, Y. *Inorg. Chim. Acta* **1987**, *128*, 245.
18. Thummel, R. P.; Lefoulon, F.; Mahadevan, R. *J. Org. Chem.* **1985**, *50*, 3824.